i) Title:

Simulation approach for the evaluation of tracking accuracy in radiotherapy; Preliminary study

ii) Authors: * Corresponding author

Rie TANAKA*[1], Katsuhiro ICHIKAWA[1], Shinichiro MORI[2], Sigeru SANADA[1]

iii) Institutions:

[1] Department of Radiological Technology, School of Health Sciences, College of Medical, Pharmaceutical and Health Sciences, Kanazawa University; 5-11-80 Kodatsuno, Kanazawa, 920-0942, Japan

[2] Research Center for Charged Particle Therapy, National Institute of Radiological Sciences; 4-9-1 Anagawa, Inage-ku, Chiba, 263-8555, Japan

iv) Running title:

Simulation approach to evaluate tracking accuracy

v) Numbers of Text pages, Figures and Tables:

Total pages	11 (including this title page)
Figures	4
Tables	0

vi) Contact information:

Phone;	+81-76-265-2537
Fax ;	+81-76-234-4366
E-mail ;	rie44@mhs.mp.kanazawa-u.ac.jp

Title

Simulation approach for the evaluation of tracking accuracy in radiotherapy; Preliminary study

ABSTRACT

Real-time tumor tracking in external radiotherapy can be achieved by diagnostic (kV) X-ray imaging with a dynamic flat-panel detector (FPD). It is important to keep the patient dose as low as possible while maintaining tracking accuracy. Simulation approach would be helpful to optimize the imaging conditions. This study was performed to develop a computer simulation platform based on a noise property of imaging system for the evaluation of tracking accuracy at any noise level. Flat-field images were obtained using a direct-type dynamic FPD, and noise power spectrum (NPS) analysis was performed. The relationship between incident quantum number and pixel value was addressed, and a conversion function was created. The pixel values were converted into a map of quantum number using the conversion function, and the map was then input into the random number generator to simulate image noise. Simulation images were provided at different noise levels by changing the incident quantum numbers. Subsequently, an implanted marker was tracked automatically and the maximum tracking errors were calculated at different noise levels. The results indicated that the maximum tracking error increased with decreasing incident quantum number in flat-field images with an implanted marker. In addition, the range of errors increased with decreasing incident quantum number. The present method could be used to determine the relationship between image noise and tracking accuracy. The results indicated that the simulation approach would aid in determining exposure dose conditions according to the necessary tracking accuracy.

Key words: Noise simulation; Image noise; Flat-panel detector (FPD); Target tracking; Radiotherapy

INTRODUCTION

Dynamic flat-panel detectors (FPDs) are commonly used in clinical practice. In external radiotherapy, real-time tumor tracking can be achieved by diagnostic (kV) X-ray imaging with a dynamic FPD [1-3]. There is concern regarding the relationship between image quality and accuracy of target tracking, because low image quality is associated with the risk of increased tracking errors, although it can reduce the patient dose. There are a number of factors that affect image quality, such as X-ray tube voltage, radiation dose, and patient body shape. In particular, reducing the radiation dose leads directly to an increase in image noise, and this may be one of the major factors reducing the accuracy of target tracking.

Recently, several methods for measuring the temporal modulation transfer function

(MTF) and the detective quantum efficiency (DQE) have been proposed, and the properties of FPDs used in dynamic imaging have been reported [4-7]. There are several reports on the performance of electric portal imaging devices [8-9]. In a previous study, it was revealed that a patient dose could be reduced by approximately 28% by optimal settings for the low-dose acquisition mode with respect to image quality and dose [10]. However, there have been no studies regarding the effects of image noise on tracking accuracy. It is necessary to address the relationship between image noise and accuracy of target tracking to keep the patient dose as low as possible while maintaining tracking accuracy.

In general, X-ray images have image noise due to statistical fluctuations in the number of incident quanta entering a detector (q) [11,12]; a higher quantum number results in less image noise. The value of q is determined as the reciprocal of the Wiener spectrum (WS) of the system (*i.e.*, q=1/WS), which is measured in flat-field images. The relationship between q and pixel value in an image is also determined from the average pixel value in the region of interest (ROI), where the WS was measured. Furthermore, q follows a Poisson distribution. Thus, images with various noise levels can be simulated by changes in the value of q and inputting them into a Poisson random number generator. The simulation images would allow us to evaluate the accuracy of target tracking at any noise level and to determine the appropriate exposure dose. Our purpose was to develop a computer simulation method to determine imaging conditions during target tracking in radiotherapy. Here, we developed a computer simulation platform based on a noise property of imaging system and investigate the feasibility of the simulation approach.

MATERIALS AND METHODS

Measurement of noise power spectrum (NPS)

(i) *Image data set*

A set of images was generated for determination of the NPS of a direct-type (a-Se/TFT) FPD system (SONIALVISION Safire2; Shimadzu, Kyoto, Japan). An RQA5 X-ray spectrum was used (HVL=7.1 mm Al, realized with 21 mm Al additional filtration at 70 kV) [13]. The matrix size was 2048×2048 pixels, the pixel size was 0.123×0.123 mm, and the field of view was 25.4×25.4 cm. Image preprocessing consisted of offset and gain correction as well as compensation for defective or nonlinear pixels, as applied in normal clinical use of the detector. Pixel scaling was linear with respect to exposure, with a bit depth of 16 bits.

(ii) *NPS determination methods*

For determination of the NPS, three independent flat-field images were obtained at each of two exposure levels (6 images in total); the exposure levels (air kerma) were 7.54 µGy and 15.7 µGy, respectively, for the two series. The air kerma values were measured free-in-air in the detector plane with an ionization chamber (AE-132a 2902209; Oyogiken Inc., Tokyo, Japan). The source-to-target distance (SID) was limited to 1.0 m in the system evaluated. The ionization chamber was placed 500 mm behind the detector, which was located approximately halfway between the X-ray tube and the detector surface. The air kerma at the detector surface was calculated by the inverse square distance law.

Regions of interest (ROIs), located manually near the detector center, were 256×256 pixels in size, with a pixel sampling pitch of 0.123 mm, in the same subarea of the full detector area, for the two series. Average pixel values were measured by use of Image-J ver. 1.42 (http://rsb.info.nih.gov/ij/) in each ROI. The NPS was calculated according to IEC6220-1-1 [14]. For removing long-range background trends, a two-dimensional 2nd order polynomial was fitted to each image and subtracted. The area of each image was divided into half-overlapping ROIs for each image and the results were averaged. The 2-D NPS was then calculated by application of the fast Fourier transform to each ROI. One-dimensional cuts through the 2-D NPS were obtained by averaging of the central ± 7 lines (excluding the axis) around the horizontal and vertical axes [15].

Creation of conversion function from pixel value to quantum number

The q is determined as the reciprocal of the WS [mm^2] of the system as follows [11,12]:

$$q = \frac{1}{WS} \tag{1}$$

In the present study, to determine q using Eq. 1, the averaged WS through all spatial frequencies in two directions were used as WS in Eq. 1 for each exposure level. The quantum number per pixel q' was then derived as follows:

$$q' = q \times ps \times ps\,, \tag{2}$$

where ps is the pixel size, which was 0.123 mm in this study. The average pixel value (in digital units) *vs.* the number of incident quanta (in count units) was fitted with a linear function, y=a+bx.

Simulation of image noise

A tracking implanted marker with an acrylic plate 20 cm thick was located in clinical settings during target tracking in radiotherapy and was imaged at 70 kV, 250 mA, 36 ms, and SID=1.0 m. An averaging image was then created from ten images obtained at the above dose as a substitute for the image with vanishingly low image noise obtained with a large dose.

Pixel values were converted to quantum number according to the conversion function. Subsequently, the resulting image was weighted from 1.0 to 0.1 in increments of 0.1. Image noise was induced by statistical fluctuation of the quantum incident to the detector, which followed a Poisson distribution. Thus, to simulate image noise, the weighted images were input into the Poisson random number generator in each pixel [11,12]. The output was the final resulting image with image noise.

Data analysis

(i) *Target tracking*

The targets in the simulation images were tracked by a template-matching technique [16]. The sum of differences in pixel value (*R*) between the search area in the next frame, $S\ (x + dx,\ y + dy)$, and the template in the current frame, $T\ (x, y)$, was expressed as follows:

$$R = \sum_{y=0}^{N} \sum_{x=0}^{M} \left| S(x + dx, y + dy) - T(x, y) \right| \quad (3)$$

$(0 < x < M,\ 0 < y < N,\ -10 < dx < 10,\ -10 < dy < 10)$

M and *N* are the size of the template, and *dx* and *dy* are the search range. The smallest *R* value was obtained when there were more similarities in the search area and template. The amount of shift (*dx*, *dy*) in the search area was determined by minimizing of *R*, and the coordinates after movement were expressed as $(x + dx, y + dy)$. In this study, the initial template was given as a region into which the target was inserted in the first frame. After the second frame, the matching region of interest in the previous frame was used as the new template. The size of the template was 50 × 50, the search range was ± 10 pixels, and thus the search area was 70 × 70 pixels, determined to cover the displacements of implanted targets.

(ii) *Evaluation method*

Tracking accuracy was evaluated in images at ten different simulated noise levels. Implanted marker was shifted in known amounts by image processing, ± 3 and ± 6 pixels in the superior-inferior and right-left directions, respectively. A total of nine patterns were assessed of each noise level, as shown in Fig. 1. The coordinates tracked were compared to the known shift amounts, and the differences were calculated as tracking errors. The maximum tracking errors were calculated and compared between simulation images at different levels of image noise.

Fig. 1

RESULTS

NPS properties

Figure 2 shows the WS in the horizontal and vertical directions for two exposure levels. The results indicated that the present system had a stable WS through all spatial frequencies, reflecting the noise property of a direct-type of FPDs. A high exposure level resulted in a higher WS than a low exposure level at all of the spatial frequencies in both horizontal and vertical directions.

Fig. 2

Conversion function from pixel value to quantum number

The average WS through all special frequencies of two directions in 7.54 μGy and 15.7 μGy were 9.57×10^{-6} mm^2 and 5.83×10^{-6} mm^2, respectively. Thus, the quantum numbers q at each exposure level were 1.05×10^{-5} mm^{-2} and 1.71×10^{-5} mm^{-2}, respectively, according to Eq. (1). The quantum numbers per pixel q' were 1.58×10^{-3} pixel^{-2} and 2.59×10^{-3} pixel^{-2}, respectively, according to Eq. (2). The fitted parameters values were a=0.0585 digital units and b=541.35 digital units per count. The quantum number per pixel q' was not zero even when the pixel value was zero due to system noise caused by the electrical circuit and system.

Effects of image noise on target tracking

Figure 3 shows the simulation images at ten different noise levels. The results indicated that a lower quantum number resulted in more image noise. It was difficult to recognize the location of the marker at quantum numbers <40%. Figure 4 shows the results regarding automatic tracking of implanted markers. There was no error in the average images without noise. The maximum tracking error increased with decreasing incident quantum number, as shown in Figure 4. In particular, the tracking error tended to increase at less than half of the original quantum number. Error bars show the standard deviation of nine data sets (n=9). The range of errors also became larger in simulation images created with smaller incident quantum numbers.

Fig. 3 Fig. 4

DISCUSSION

Image noise has a big effect on visualization of an object with low contrast like a target in radiotherapy. The present method was able to provide the relationship between image noise levels and tracking accuracy. The maximum tracking error increased with increases in the image noise. The range of errors also increased with increasing image noise. In this study, the tracking error gradually increased about after half of the original quantum number. It was actually difficult to identify implanted markers in images generated by less than half of the original incident quantum number. Such information would be very useful for physicists to determine the exposure dose according to the necessary tracking accuracy. The present method could be applied to a different FPD system, requiring only the determination of the conversion function for that system. These results indicated the feasibility of the simulation approach for determination of the exposure dose during a real-time target tracking in radiotherapy.

However, there are several limitations that need to be solved in the present method.

For example, there are the other factors that affect image quality, such as X-ray tube voltage, image lag, image blurring, and patient body thickness. In addition, it is necessary to consider the other noise factors except quantum noise, such as electrical noise and structural noise. It should be highlighted in this context that the simulation approach allows us to evaluate the accuracy of target tracking at any noise levels. However, all of the noise factors are not involved in the simulation image at the present time. For clinical implementation, further studies are required to expand the system considering the other factors and to evaluate it in a real moving target in clinical cases.

CONCLUSION

The present study was performed for development of a computer simulation method for determining imaging conditions during target tracking in radiotherapy. Image noise was simulated based on the noise property of that system, and the simulation was able to provide the relationship between image noise levels and accuracy of target tracking, which the maximum tracking error increased with decreases in the incident quantum number. These results indicated the feasibility of the simulation approach for determination of the exposure dose during a real-time target tracking in radiotherapy.

REFERENCES

1. Jaffray DA, et al (2002) Flat-panel cone-beam computed tomography for image-guided radiation therapy. Int J Radiat Oncol Biol Phys. 53:1337-1349.
2. Moore CJ, et al (2006) Developments in and experience of kilovoltage X-ray cone beam image-guided radiotherapy. Br J Radiol. 79:66-78.
3. Huntzinger C, et al (2006) Dynamic targeting image-guided radiotherapy. Med Dosim. 31:113-125.
4. Overdick M, Solf T and Wischmann H (2001) Temporal artifacts in flat dynamic x-ray detectors. SPIE medical imaging. Proc. SPIE. 4320:47-58.
5. Friedman SN, and Cunningham IA (2006) A Method to measure the temporal MTF to determine the DQE of fluoroscopy system. SPIE medical imaging 2006, Proc. SPIE. 6142:61421X-1-61421X-11.
6. Friedman SN, and Cunningham IA (2009) A small-signal approach to temporal modulation transfer functions with exposure-rate dependence and its application to fluoroscopic detective quantum efficiency. Med Phys. 36:3775-85.
7. IEC (2008) IEC International standard 62220-1. Medical diagnostic X-ray equipment-Characteristics of digital imaging devices-Part 3: Characteristics of digital X-ray imaging devices-Part 1-3: Determination of the detective quantum efficiency – detectors used in dynamic imaging. Geneva, Switzerland
8. Cremers F, et al (2004) Performance of electronic portal imaging devices (EPIDs) used in radiotherapy: image quality and dose measurements. Med Phys. 31:985-96.
9. Berger L, et al (2006) Performance optimization of the Varian aS500 EPID system. J Appl Clin Med Phys. 7:105-14.
10. McGarry CK, Grattan MW, Cosgrove VP (2007) Optimization of image quality and dose for Varian aS500 electronic portal imaging devices (EPIDs). Phys Med Biol. 52:6865-77.
11. Dainty JC, and Shaw R (1974) Image Science. London, UK: Academic Press
12. Walter H. Review of radiologic physics (3rd edn) (2010) Philadelphia, USA: Lippincott Williams & Wilkins
13. IEC (1994) IEC International standard 61267 Medical diagnostic X-ray equipment-Radiation conditions for use in the determination of characteristics. Geneva, Switzerland: IEC
14. IEC (2003) IEC International standard 62220-1. Medical diagnostic X-ray equipment-Characteristics of digital imaging devices-Part 1: Determination of the detective quantum efficiency. Geneva, Switzerland: IEC

15. Neitzel U, et al (2004) Determination of the detective quantum efficiency of a digital x-ray detector: Comparison of three evaluations using a common image data set. Med Phys. 31;8:2205-2211.
16. Ballard DH, Brown CM. Computer vision (1982) Englewood Cliffs, New Jersey: Prentice-hall.

Funding
This work was supported in part by a research grant from Japanese society of medical physics (JSMP).

Figure legends

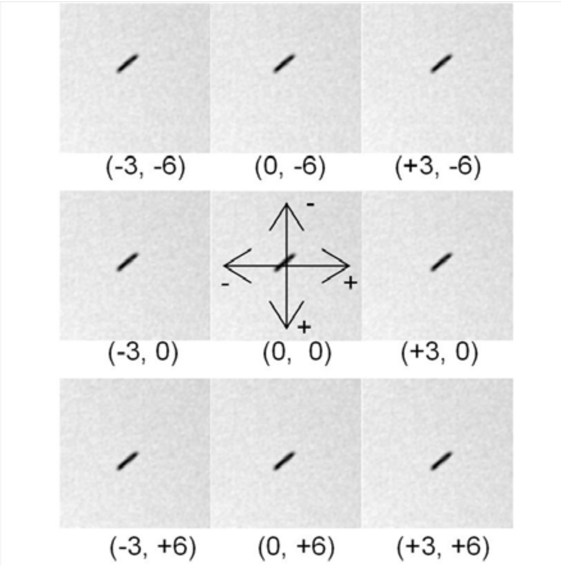

Fig. 1 Markers were shifted in nine combinations of ± 3 and ± 6 pixels in superior-inferior and right-left directions, respectively.

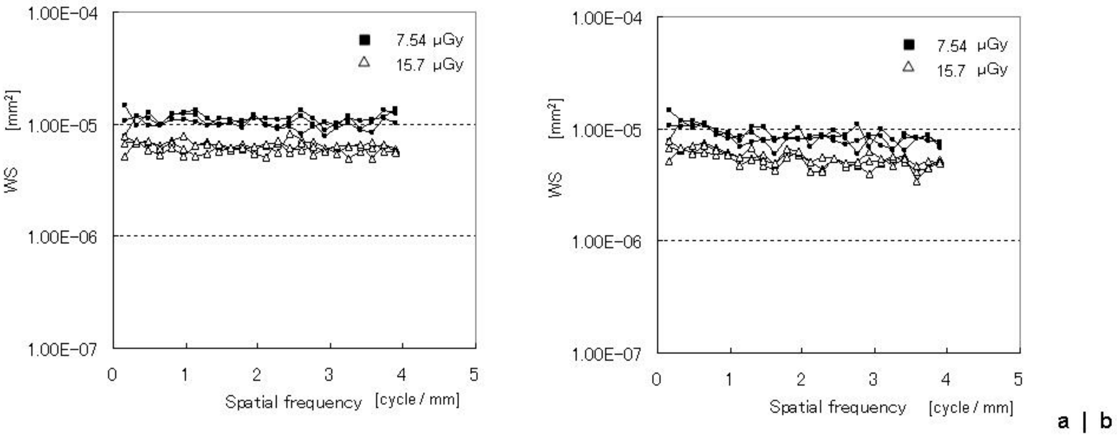

Fig. 2 Noise power spectra as determined for the set of flat-field images at two noise levels. (a) Horizontal direction. (b) Vertical direction.

Fig. 3 Simulation images at ten different noise levels. (a) Averaging image (*i.e.*, image without noise). (b)–(k) Images with simulated noise by decreasing the number of incident quanta by 10%. Image noise increased as the incident quantum number decreased.

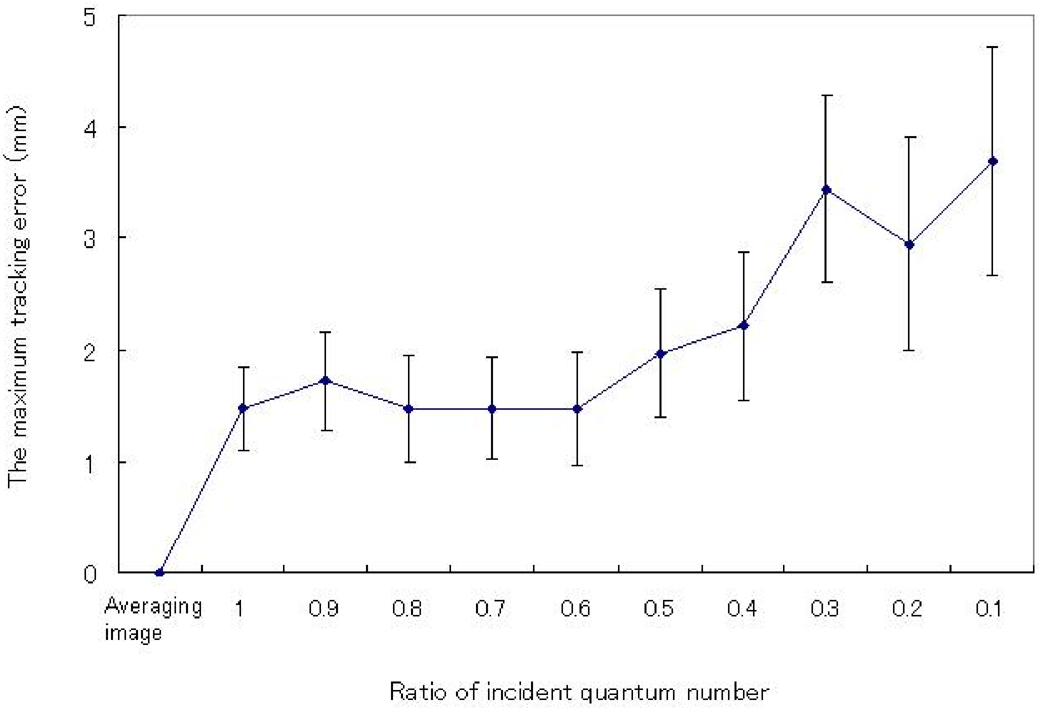

Fig. 4 Relationship between the maximum tracking error and ratio of incident quantum number to FPD (flat-field image). The average image without noise has no error, while, there are tracking errors in the images simulated in ratio of incident quantum number from 1.0 to 0.1. Error bars show ±SD. (SD: standard deviation, n=9)